A Novel Method of Fault Location for Single-Phase Microgrids

Jiajun Duan, *Student Member*, *IEEE*, Kaifeng Zhang, *Member*, *IEEE*, and Liang Cheng, *Member*, *IEEE*

***Abstract*—This paper presents a novel fault location method for single-phase microgrids. In order to locate a fault, a feature specific to the fault location is found, namely the maximum oscillation magnitude of the transient voltage signal induced by the fault. Our theoretical study and extensive simulations demonstrate that there is an approximated linear relationship between the maximum magnitude of the transient signal observed by a sensor and the distance between the sensor and the fault location. Based on the discovered relationship, microgrid topology and sensor location information, we have designed an algorithm capable of locating the fault in the single-phase microgrids. The proposed fault location method has been implemented and validated through simulations in Electro-Magnetic Transient Program (EMTP) and MATLAB. The average localization error is less than 9% in the evaluation results, which manifests the significance of the novel method as there is little research done for fault location in single-phase microgrids.**

***Index Terms*—Single-phase microgrid, Fault location, Transient signal, Distributed generators**

I. Introduction

MICROGRID is "a group of interconnected loads and distributed energy resources (DERs) within clearly defined electrical boundaries that acts as a single controllable entity with respect to the grid" [1]. According to the U.S. Department of Energy (DOE), microgrid has drawn increasing attention in recent years because it has many advantages such as utilizing green energy resources, offering flexible operations, promoting reliability and resilience when utility grids experience disturbances [2].

Based on the number of grid phases, microgrids can be categorized as three-phase systems and single-phase systems. Three-phase microgrids have been studied by many researchers and installed in utility power grids [3]. Meanwhile, single-phase microgrids are applicable to power systems with relatively small power and low voltage levels, such as residential house, small commercial lot, ship, space station, minor military base, or island scenarios [4]-[5].

This work was supported in part by the U.S. Department of Energy under Grant DE-OE0000428. Any opinions, findings, and conclusions expressed in this paper are those of the authors and do not necessarily reflect the views of the sponsors of the research.

Jiajun Duan is with the Department of Electrical Engineering, Lehigh University, Bethlehem, PA 18015 USA (e-mail: jid213@lehigh.edu).

Kaifeng Zhang is with the Department of Computer Science and Engineering, Lehigh University, Bethlehem, PA 18015 USA, on leave from School of Automation, Southeast University, Nanjing 210096 China with the support by the China Scholarship Council (e-mail: kaifengzhang@seu.edu.cn).

Liang Cheng is with the Department of Computer Science and Engineering and Laboratory of Networking Group (LONGLAB), Lehigh University, Bethlehem, PA 18015 USA (e-mail: cheng@cse.lehigh.edu).

This paper focuses on solving the problem of fault location in single-phase microgrids. In each hierarchy of power grid, from transmission, distribution to microgrid, fault location is an important problem. Thus a good amount of fault location methods have been studied by researchers.

A. Related Work

Fault location in transmission networks generally assumes a long transmission line with sensors deployed at either one or both ends of the line. The Travelling Wave (TW) method utilizes the time difference between the incidence wave and the reflection wave of transient voltage/current signals caused by disturbance to identify the fault location [6]-[7]. The TW method is also the key method suggested by the IEEE guide for fault location on AC transmission and distribution lines [8]. The authors in [6] propose a solution to detect small-voltage-magnitude faults that happen very close to the sensors or when a single phase is grounded.

Fault location in distribution networks is usually accomplished based on the information collected by one main sensor. Distribution networks often have relatively smaller scales and more complicated topologies compared to transmission networks. The typical topology of distribution networks is a tree with the main sensor installed at the root of the tree, namely the distribution substation. The Wavelet Transform (WT) method in [9] is introduced to find the fault branch. Its theoretical foundation depends on the high frequency components of transient signals which may have different performances with respect to the different paths they pass through. Based on this idea, in [10] researchers consider that there is a characteristic frequency corresponding to a certain location of distribution networks. The fault location can be determined by comparing the theoretical frequency with the frequency identified by the WT. However, the characteristic frequency is related to many other factors in practice which can be easily disturbed. In [11], high frequency components (10^3-10^9 Hz) are first extracted by the WT. Then the fault distance is calculated by the TW method which increases the noise immunity. There still exist other methods, e.g. [12], which require a precise simulation to calculate the fault location.

One of the main problems when trying to use aforementioned methods in a microgrid is that these methods need data acquisition devices with fairly high sampling rates to achieve the high resolution in fault location needed for the microgrid. For example, in the traveling wave approach [9], it needs to detect the time difference between the first transient wave and the second transient wave arriving at the sensor; in the transmission line case the time difference is in a magnitude of seconds corresponding to a wave traveling distance of about 100 Km while in a microgrid the time difference would be in a magnitude of 10^{-6} to 10^{-7} seconds If such concept would still apply. Thus, for a three-phase microgrid, new methods including frequency shift [13], phase shift [14], high impedance detection [15] and harmonic current injection [16] have been developed. These methods take three-phase symmetric components as their basic features and are capable working in both transmission networks and distribution networks. Other fault location methods use data mining and d-q WT approach respectively [17]-[18]. They are both specifically designed for three-phase microgrids.

B. Uniqueness and Contribution of Our Research

To the best of our knowledge, little research about fault location in single-phase microgrids has been done up till now. The obvious difference between single-phase microgrids and transmission, distribution and three-phase microgrids makes this work full of challenges.

1) Three-phase related features such as unbalance attribute components are no longer available. This requires us to discover new features that may be used for fault location in single-phase microgrids.
2) The relatively small scale of microgrid leads to a great difficulty for existing methods to extract features from fault signals to locate the fault as the features still overlap with each other during the short propagation distance of the signals. Only monitoring devices with quite high sampling frequencies could offer data to fulfill the feature extraction requirement with prohibitive cost with respect to microgrids deployments if such data processing algorithms would be available.

Therefore, in our research we explore various features available in single-phase microgrids and investigate their relationship with the fault patterns. Based on extensive simulations we have discovered a new feature and its relationship with fault location and designed a novel approach for solving the fault location problem for single-phase microgrids based on information fusion from multiple sensors. We have validated the approach with theoretical and simulation studies. The major contributions of this paper include:

1) Revealing the approximated linear relation between the magnitude of transient signals and the fault distance in single-phase microgrids. When a short-circuit fault occurs, voltage sensors should detect an oscillating transient signal. The longer the distance between the sensor and the fault location, the larger the magnitude of the transient signals sensed.
2) Designing an appropriate algorithm for fault location based on the newly discovered relationship and evaluating the performance of the algorithm including its error analysis and robustness analysis. The average localization error is less than 9% in the evaluation results, which manifests the significance of the novel method as there is little research done for fault location in single-phase microgrids.

The remainder of this paper is structured as follows. Section II presents the fault location problem and introduces the proposed approach; Section III establishes the theoretical foundation of the novel approach; Section IV describes the designed algorithm. In order to demonstrate the correctness of the algorithm, Section V presents the simulation design of four cases and their results including error analysis and robustness evaluation of the algorithm; Section VI concludes the paper.

II. ProblemStatement and Proposed Approach

A. Problem Statement

Without loss of generality, in order to satisfy microgrid stability requirements such as those prescribed by IEEE1547, we assume that a microgrid has a control center or a centralized SCADA/energy management system that collects sensor data and adjust operation states of the microgrid [19]. Generally the protective relays are installed at DGs and important loads and there is no protection device for each transmission line in such microgrids. Therefore it may be labor-intensive and time-consuming to locate a fault that has happened in a transmission line spanning hundreds of meters that may be hard to inspect. As shown in Fig. 1, we also assume that each distributed generator (DG) in the microgrid has a data acquisition device, and there is also a data acquisition device installed at the interface between the microgrid and the external grid. In Fig. 1, dotted lines denote information flows sent from sensors to the central controller and dash lines represent the control signal flows from the central controller to the DGs. Each circuit line is marked as T_i. As mentioned in [20], centralized control performs well in microgrids and is not difficult to realize while there also exist microgrids adopting decentralized control. In this paper, we focus on microgrids with centralized control and the decentralized control scenarios will be our future research work.

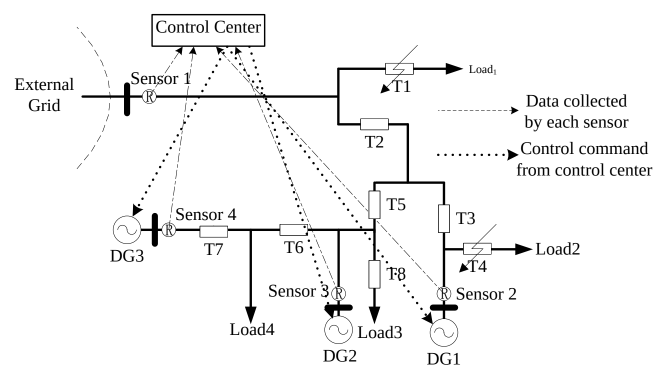

Fig. 1. Microgrid with centralized control.

In general, for the problem of fault location in single-phase microgrids, the following prerequisites are used.

1) The microgrid topology is known.
2) The basic system parameters are known. For instance, the accurate line length and approximately the equivalent impedances of circuits.
3) The basic circuit principles and theorems are applicable, such as Ohm's Law, Kirchhoff's law, and Thevenin's theorem.
4) The electrical signals can be sampled by multiple sensors in the microgrid at the same time.

The fault location problem in single-phase microgrids is to estimate the fault position based on the aforementioned information and the error between the estimated fault location and the actual fault location should be within an engineering tolerance margin. For example, assume that a short circuit has occurred at the midpoint of transmission line 4 (T4) in the microgrid shown in Fig. 1. The transient voltage signal caused by the short circuit has been sensed by Sensor 1 through Sensor 4. Using the sensor data along with the known topology and system parameter information, a fault location solution should be able to estimate that the fault has happened at somewhere close to the midpoint of T4. The error between the estimated fault location and the actual fault location should be within an engineering tolerance margin.

B. *Revisiting Fault Location Methods for Different Domains*

Due to the lack of three-phase parameters, fault location for single-phase microgrids has a great constraint on its effective information available. As transmission networks and distribution networks are three-phase systems, many of their fault location methods use symmetric three-phase components to solve the problem. However, those methods are not directly applicable in the single-phase microgrid that does not have any three-phase components.

Moreover, a typical microgrid runs across several hundred meters, which results in discrepancies between microgrids and other networks in terms of network complexity, geographical coverage, and system parameters.

The fault location problem of a transmission network concerns about a group of long cables or overhead lines. In the transmission network, sensors are usually deployed at one or two sides of the transmission line. If there are sensors installed at both ends, a precise synchronism device is required to support the synchronized sampling function. The long length of a transmission line provides comparatively accurate circuit parameters and also warrants a recognizable resolution of signal features to be extracted.

Because of these differences, fault location methods in transmission networks cannot be directly applied in the microgrid. The features used in those methods overlap due to microgrid's short electrical distance. For example, the TW method [9] calculates the fault location via the time difference between the first transient wave and the second transient wave arriving at the sensor using the following formula:

$$t = 2 \cdot (L - l) / v \tag{1}$$

where L is the total transmission length, l is the distance between the fault location and the sensor, v is the propagation velocity of the transient wave which is close to the light velocity, namely $3 \cdot 10^8$ m/s. As the length of microgrid is generally about several hundred meters, the data acquisition devices would have to be able to discriminate two different features within 10^{-6} to 10^{-7} seconds should the above-mentioned approach based on (1) be applied. The sampling rate of an analog to digital conversion should be in dozens of gigabit per second to extract the feature, which would not be feasible in a typical microgrid deployment.

The fault location problem in a distribution network is often based on a tree or radial topology. The main monitoring devices are generally installed at the interface of the distribution substation. Because it depends on the single sensor to determine the fault location and fault type, the data acquisition devices need quite high sampling rate. To compare the current sampling information with existing information in the database is an effective way to identify fault location.

The fault location methods for distribution networks lose their effectiveness in single-phase microgrids too. The main reason is still the problem of features getting overlapped because of the short electrical distances and sensor limitations.

Therefore the practical engineering requirements motivate us to develop a new fault location method which is specifically designed for the single-phase microgrids.

C. *Proposed Approach*

We believe that the essence in solving the fault location problem in single-phase microgrids is to find a feature which corresponds to the distance from the fault location to the sensor. Thus we conduct theoretical studies and simulation experiments seeking such features. The detailed theoretical derivation is presented in Section III.

The simulations of short circuit in single-phase microgrids are performed in the Electromagnetic Transients Program (EMTP). After analyzing data collected by each sensor deployed at every important node, we find that the basic electrical signals are impacted by the fault occurrence. The changes in current and frequency are difficult to distinguish. Nevertheless, the transient signals of voltage present an observable pattern with different fault locations.

Take the microgrid in Fig. 1 as an example. When a short circuit occurs at the transmission line 1 (T1), the zoom-in view of transient voltage signals received by the four sensors during the fault period are plotted in Fig. 2. If the fault occurs at the transmission line 4 (T4), the zoom-in view of transient voltage signals are plotted in Fig. 3. It can be seen that an abrupt change of voltage at the fault point results in oscillating transient signal fluctuations. The closer a sensor sits from the fault location the smaller the magnitude of the transient signal it observes. In other words, the magnitude of the transient voltage signal becomes larger when the distance between the sensor and the fault location is longer.

Extensive simulation data presented in Section IV show that the maximum magnitude of transient signals is proportional to the distance between the fault and the sensor. Let y represent the maximum magnitude of transient signals, and x is the distance between the fault location and the sensor. Then the

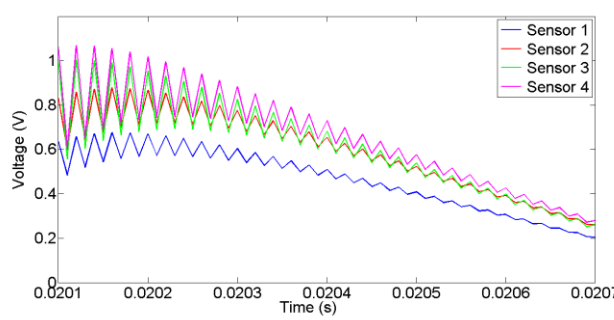

Fig. 2. Zoom-in view of transient voltage signals caused by a short circuit at T1 in a microgrid depicted as Fig. 1 during fault time.

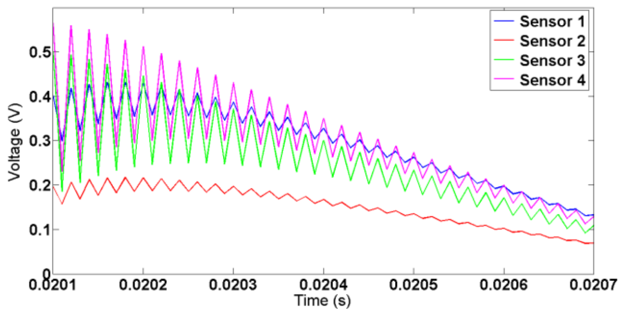

Fig. 3. Zoom-in view of transient voltage signals caused by a short circuit at T4 in a microgrid depicted as Fig. 1 during fault time.

relationship between y and x approximate a linear function:

$$y = a \cdot x + b \tag{2}$$

where a and b are constant coefficients associated with each specific microgrid.

The general process of our fault location method can be summarized as follows:

1) The transient signals are detected by each sensor and the data are input to the algorithm.
2) Possible fault locations are estimated by the algorithm with known information, including the above-mentioned linear relationship, the microgrid topology and the system parameters such as the length of each circuit.
3) The possible fault locations are ranked based on the comparison between the calculated magnitude of the transient signal and the actual magnitude observed by sensors.
4) The coefficients in the linear relationship are calibrated using the information of the actual fault location found based on the estimated fault location.

Besides the significance of the discovered relationship for the fault location method, another merit of our research is that it takes advantage of multi-sensor availability in a microgrid. The detailed method derivation, illustration, and validation are described in the following sections.

III. Theoretical Analysis

This section analyzes the principle supporting the discovered relationship mentioned above. The full-scale theoretical analysis of a typical microgrid as depicted in Fig. 1 is a daunting challenge. Thus we simplify the short circuit situation of the microgrid as an equivalent circuit shown in Fig. 4. Z_{ex} is the equivalent impedance of the external grid. Z_1 is the transmission line impedance in series with similar small short ground impedance which represents different short circuit distances. For example, assume that a short circuit occurs at T1 in Fig. 4. When observing from Sensor1, its left side is equivalent to a combination of input voltage and external impedance denoted as V_{in} and Z_{ex}. For its right side, the only remaining part after short-isolated is the impedance from the sensor to the fault location in series with short ground impedance marked as Z_1. The output voltage V_{out} is the voltage that applied on Z_1. Similarly, a one-port equivalent circuit of short line can be obtained from the port of any other sensors. In this paper, we use the simple switching transient analysis by Laplace transform for post-fault states [21] to illustrate that different fault positions will cause different transient behaviors. Note that the feature used in our approach is extracted during the post-fault stage where there is no topology change.

$$H(s) = \frac{X_1}{X} + \left(\frac{R_1}{X} - \frac{R \cdot X_1}{X^2}\right) \Big/ \left(s + \frac{R}{X}\right) \tag{3}$$

$$H(t) = \frac{X_1}{X} \cdot \delta(t) + K \cdot e^{-\frac{R}{X}t} \tag{4}$$

where $X = X_1 + X_{ex}$, $R = R_1 + R_{ex}$, $K = \frac{R_1}{X} - \frac{R \cdot X_1}{X^2}$ and $\delta(t)$ is an impulse function. Generally in the low voltage level grids (e.g. below 110kV), the resistance weighs more than the reactance. Thus, if the input voltage is a sinusoidal function of frequency, the output voltage is an oscillated attenuating signal. Fig. 5 presents examples of the transient voltage response when R_1=0.04, 0.06, 0.08 and 0.1 ohm, $X_1=10^{-4}$ ohm, R_{ex}=5 ohm and X_{ex}=0.4 ohm. The influence of the resistance on the maximum magnitude of the oscillation signal is obvious: the larger the resistance, the larger the maximum magnitude.

From the derivation shown above, it can be concluded that the magnitude of the transient response is proportional to R_1, i.e. proportional to the electrical distance if the circuit line is homogeneous. Therefore the discovered relation between the magnitude of transient voltage signals and the distance between the sensor and the fault location has its theoretical support, which builds the foundation for the fault location algorithm design described in the next section.

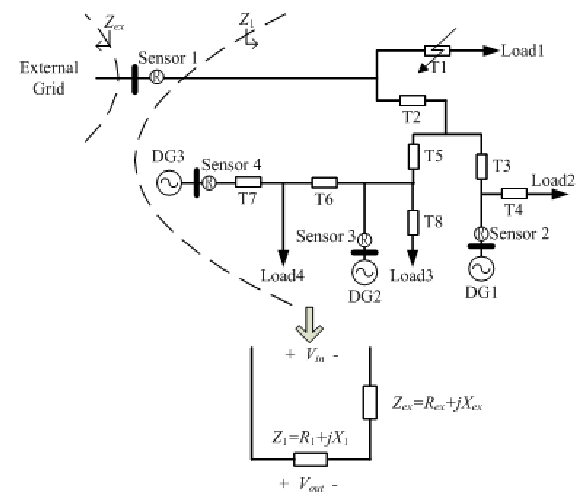

Fig. 4. Equivalent circuit of a short circuit.

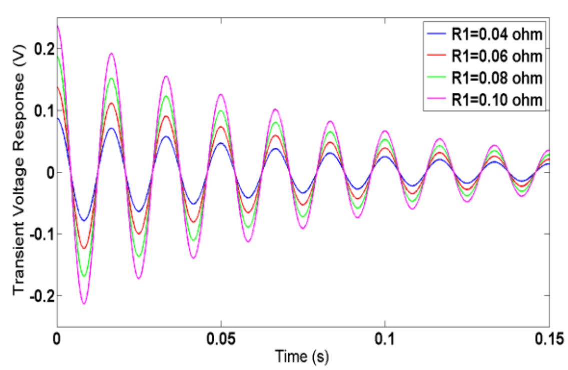

Fig. 5. Output waveform of the equivalent circuit.

IV. Algorithm Design

The major objective of running a fault location method is to provide fault position estimations for the microgrid maintenance staff to efficiently locate and eliminate the fault when it happens. In this paper we differentiate two different types of fault position in the microgrid. One type is called an internal circuit fault (ICF) which has sensors deployed at both sides of the line where the fault occurs, e.g. T2 in Fig. 1. The other type is a called load side fault (LSF), meaning that a fault occurs at the load side, e.g. T1 in Fig. 1.

A. Data Acquisition

After a fault occurs, the data collected by each sensor during the fault period will be acquired as the input to the algorithm.

B. Fault Distance Calculation

By analyzing transient signals collected by the sensors, the algorithm identifies the sensor that has observed the smallest magnitude of the transient signals as the closest one to the fault location. As shown in Fig. 6, if we assume that there are n sensors in a single-phase microgrid and the fault spot is x meters away from the closest Sensor i, the distance between the fault location and any sensor j can be expressed using x and d_{ij}, i.e. the distances between Sensor i and Sensor j, as ($d_{ij}+x$) or ($d_{ij}-x$); the plus or minus sign corresponds to the load side fault (LSF) or the internal circuit fault (ICF) defined above. Thus the relationship between the maximum magnitude of the transient signals and the fault location can be expressed as (5).

$$\begin{cases} y_i = a \cdot x + b \\ y_j = a \cdot (d_{ij} \pm x) + b \end{cases} \qquad [j \in n, j \neq i] \tag{5}$$

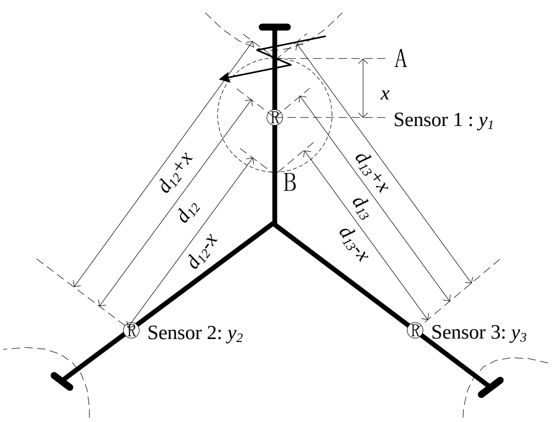

Fig. 6. Fault location schematic diagram.

We first assume that the fault is an ICF and use the minus sign to derive x. In fact if there are more than two sensors in the microgrid we may obtain an over-determined equation set as each sensor data can provide an equation based on (5). The method of left division may be used to find an approximate solution of x.

The calculated x only indicates an approximate location estimation if the fault is a load side fault. That is why the algorithm needs to rank the possible fault locations estimated to offer more information to the microgrid maintenance staff.

C. Fault Location Ranking

Based on the calculated distance x between the fault location and the nearest sensor, we can generate a list of possible fault locations by finding the intersections of a circle centered at the sensor with a radius of x and the related circuit lines. For example, as shown in Fig. 6, the possible fault locations corresponding to the Sensor 1 (i.e. the nearest sensor to the fault according to the smallest magnitude of the transient signals observed by the sensors) include point A and point B. Then we need to decide whether the fault is more of a LSF type at point A or more of an ICF type at point B. We plug the calculated value of x back into (5) and use the plus sign corresponding to a LSF and the minus sign corresponding to an ICF to calculate the values of y respectively. Then we compare the calculated values of y with the detected values y_i using the root-mean-square error (RMSE) in both LSF and ICF cases. For example,

$$RMSE = [\sum_{i=1}^{n} (y - y_1)^2 / n]^{\frac{1}{2}} \tag{6}$$

The case with a smaller RMSE has a higher ranking than the case with a larger RMSE so that we are able to decide which estimated fault location has a higher possibility to be close to the actual fault location.

D. Coefficient Calibration

After the fault location is found, the actual fault distance and magnitude can be visualized along with history data in the coordinate system as illustrated in Fig. 6 and a new line of (2) can be computed that minimizes the fitting error, e.g. using the least square approach. Thus, the function coefficients a and b in (2) get calibrated in every fault case which may help (2) reflect the characteristics of the microgrid more and more accurately.

Although the accurate values of the coefficients a and b are unknown at the first time of fault occurrence, they can be estimated roughly by simulations of the microgrid. For example, as simulation results of a microgrid listed in Table II in the next section we can set a=0.001 and b=0.1 by their corresponding order.

The fault location algorithm's flow chart for one round of fault location is summarized in Fig. 7.

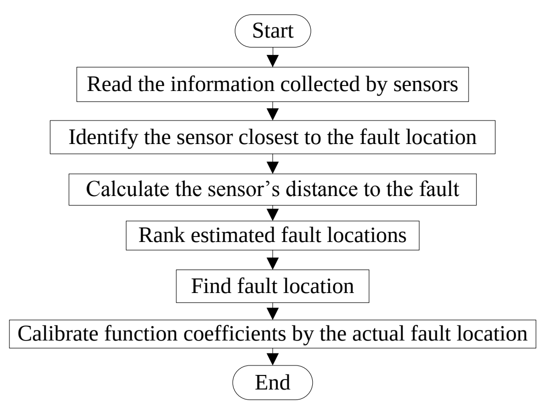

Fig. 7. Flow chart of the algorithm.

V. Simulation and Result Analysis

A. Simulation Design

We use the Electromagnetic Transient Program (EMTP) for power system simulation and MATALB for analyzing and processing data. The simulation of short circuit faults is conducted in a simulated in Fig. 1, which shows a typical microgrid topology [12]. Referring to what has been done in [10] and [12], we set all the generators be represented by stable voltage sources. The external grid has a smaller source impedance compared with those DGs. The short circuit situation is simulated by a grounded switch and the grounded impedance is represented by the resister, inductor and capacitor in series and parallel. Simulations and analyses are performed corresponding to different short circuit positions in the microgrid.

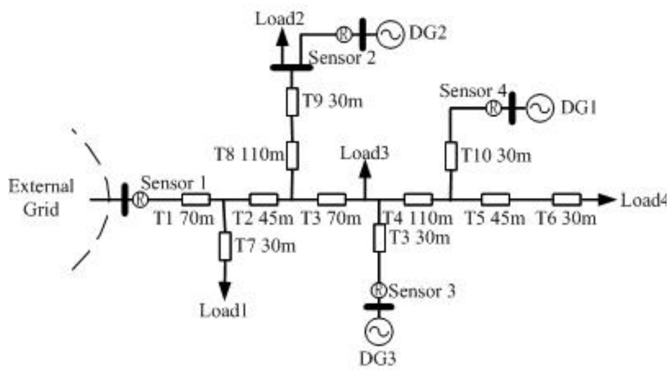

Fig. 8. Simulation topology, microgrid B.

The circuit line is simulated based on the distributed parameter model. We apply two parameter set (A and B) and the resistances, inductances, and capacitances per unit length of set A are R_1=0.2 Ω/km, L_1=0.004 H/km and C_1=5.7e-6 F/km. For the set B: R_2=0.1 Ω/km, L_2=0.002 H/km and C_2=2.85e-6 F/km. Readings of all the voltage sensors installed are available in real-time.

We also conduct simulation using another microgrid topology (Microgrid B) depicted in Fig. 8.

The four cases reported here are listed below:

1) Case 1: Microgrid A, 220v, parameter set A
2) Case 2: Microgrid A, 110v, parameter set A
3) Case 3: Microgrid B, 110v, parameter set A
4) Case 4: Microgrid A, 110v, parameter set B

B. Main Simulation Results

The simulation results in this section contain two parts. The first part demonstrates the linear relationship (2) between the magnitude of the transient signal and the fault distance. The second part shows the algorithm and its performance.

To explore the internal characteristics of the microgrid, the short circuit is tested on the microgrid every 10 meters. Then the data collected by EMTP would be analyzed via MATLAB.

The result of the relationship between the fault distance and the maximum magnitude of transient signal has been plotted in Fig. 9 (a), (b), (c), and (d), where x axis shows the fault distance and y axis shows the maximum magnitude of transient signal.

Using the Curve Fitting Toolbox of MATLAB to fit the data with candidate curves, we have observed that overall the linear function enjoys smaller root mean square error than the exponential as shown in Table I. This result matches our theoretical study.

TABLE I
Curve Fitting Results

	Exponential $y=a\cdot exp(b*x)$	RMSE	Linear $y=a\cdot x+b$	RMSE
Case 1	a=0.4909 b=0.00349	0.207	a=0.004105 b=0.2575	0.161
Case 2	a=0.2455 b=0.003489	0.104	a=0.002052 b=0.1288	0.086
Case 3	a=0.186 b=0.004032	0.065	a=0.001548 b=0.09403	0.066
Case 4	a=0.1617 b=0.002909	0.044	a=0.000925 b=0.1222	0.041

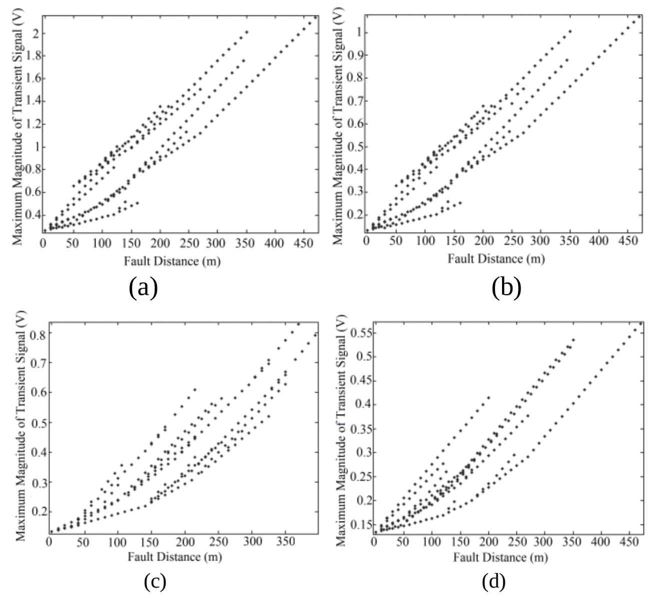

Fig. 9. The relation between transient signal magnitude and fault distance: (a) a 220v microgrid with topology A and parameter set A (Case 1); (b) a 110v microgrid with topology A and parameter set A (Case 2); (c) a 110v microgrid with topology B and parameter set A (Case 3); (d) a 1100v microgrid with topology A and parameter set B (Case 4).

We have also observed that the coefficients in the function are proportional to the voltage level as shown in Fig. 9 (a) and Fig. 9 (b): they have the same performance except the magnitude. They are also affected by both line parameters and the microgrid topology. In the second part of simulation results, Case 2 listed above is used as an example to demonstrate the algorithm and its analysis.

TABLE II
The Relation Between Fault Distance and Magnitude of Transient Voltage Signal

Sensor	Sensor 1	Sensor 2	Sensor 3	Sensor 4
Magnitude (V)	0.1674 (30 m)	0.2872 (115 m)	0.4468 (120 m)	0.5111 (240 m)
Distance (m)	x	145±x	150±x	270±x

When a fault occurs at T2 in the microgrid of Fig 1, i.e. 30 meters away from Sensor1, the maximum magnitude of oscillating voltage signals detected by each sensor is shown in Table II. It can be seen that the sensor installed at the interface of external gird gets the minimum magnitude. Therefore we assume that the fault position is x meters away from this sensor.

Then, the distance between the fault and other sensors can also be expressed with x.

Based on the discussions in Section II and the data from Table II, we obtain the functions equations:

$$\begin{cases} 0.1674 = a \cdot x + b \\ 0.2872 = a \cdot (145 - x) + b \\ 0.4468 = a \cdot (150 - x) + b \\ 0.5111 = a \cdot (270 - x) + b \end{cases} \tag{7}$$

These equations are over-determined and the specific solution can be found by the left division method: x equals 39.37 meters. Based on the values of x, a, and b, the RMSE of the calculated transient voltage magnitude and the measure magnitude will be 0.3095V if the fault is assumed to be an ICF. If we assume an LSF, then the RMSE is 0.1895V. Theoretically, a smaller RMSE value means that it is closer to the real situation. In this example, however, due to the impact of the initial value setting of the unknown factors a and b, the ranking result for the first fault occurrence of this time is not correct. When the actual fault location is found, the values of a and b in (5) will be calibrated. In this case, a=0.0016 and b=0.15. When faults occur in the second time and later, the ranking results will become more and more accurate with the calibrated coefficients. Table III shows a series of fault location results when it is an ICF at the first time. Table IV shows the situation when it is an LSF at the first time.

TABLE III
FAULT LOCATION RESULTS WITH ICF IN THE FIRST TIME

Fault occurrence (Fault type)	Actual fault location	Calculated/Estimated fault location	Ranking result (RMSE)	Calibration of coefficients *a* and *b*
First time (ICF)	30 m (away from Sensor1, ICF)	39.37 m	1. LSF (0.1895) 2. ICF (0.3095)	a= 0.0016 b=0.15
Second time (ICF)	25 m (away from Sensor4, ICF)	22.52 m	1. ICF (0.1253) 2. LSF (0.1646)	a= 0.0017 b=0.16
Third time (LSF)	10 m (away from Sensor3, LSF)	9.23 m	1. LSF (0.2062) 2. ICF (0.2207)	a=0.0017 b=0.17

TABLE IV
FAULT LOCATION RESULTS WITH LSF IN THE FIRST TIME

Fault occurrence (Fault type)	Actual fault location	Calculated/Estimated fault location	Ranking result (RMSE)	Calibration of coefficients *a* and *b*
First time (LSF)	50 m (away from Sensor1, LSF)	41.40 m	1. LSF (0.4918) 2. ICF (0.6200)	a= 0.0016 b=0.22
Second time (LSF)	20 m (away from Sensor4, LSF)	16.52 m	1. LSF (0.1493) 2. ICF (0.2189)	a= 0.0016 b=0.18
Third time (ICF)	30 m (away from Sensor2, ICF)	32.87	1. ICF (0.0140) 2. LSF (0.2263)	a=0.0019 b=0.15

It can be seen clearly from the algorithm results that, except for the ICF at the first time, the ranking results find the correct fault type, ICF or LSF. Meanwhile, there is a tiny difference between the calculated distance and the real distance. In the following subsection, we focus on the error analysis of this method.

C. Error Analysis

Fault location error for any fault is calculated by (8), which has also been used in other research such as [10]. For each case listed in subsection V.A, we have tested 260 fault locations and taken the mean value of the errors of each fault location estimation as shown in (9). The error results are listed in Table V showing an average error in the range between 7% and 9%.

$$Error = (L_{Est} - L_{Act})/L_{Tol} \cdot 100\% \tag{8}$$

$$Error = Mean(|L_{Est} - L_{Act}|)/L_{Tol} \cdot 100\% \tag{9}$$

where L_{Est} is the estimated fault location, L_{Act} is the actual fault location and L_{Tol} is the length of total section.

TABLE V
ERROR ANALYSIS RESULTS

	Mean error distance (m)	Line Length (m)	Error
Case 1	35.7369	470	7.6%
Case 2	35.1365	470	7.48%
Case 3	34.3152	395	8.69%
Case 4	33.8493	470	7.2%

D. Robustness of the Proposed Algorithm

As the load fluctuations may introduce some noise and influence the transient signal detected, we have conducted simulations under load fluctuation conditions to evaluate the robustness of the proposed fault location method. Load 1, Load 2 and Load 3 changes smoothly from 100+0.1j Ohms to 120+0.05j Ohms, 110+0.008j Ohms and 90+0.02j Ohms respectively.

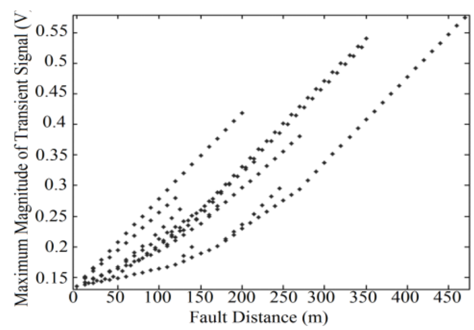

Fig. 10. Simulation result of Case 4 with load fluctuation.

The simulation results of Case 4 with the load fluctuations described above is shown in Fig. 10. It can be observed that Fig. 9 (d) is almost the same as Fig. 10 which is hard to be discriminated by human eyes. But the curve fitting and error analysis results shows the robustness of the algorithm under noise disturbance that the error only increases 0.05% with 10-20% changes in the load.

VI. Conclusion

Microgrid has drawn increasing attention in recent years while there is little research on fault location solutions for single-phase microgrids. The difference between a single-phase microgrid and other transmission, distribution and three-phase microgrids makes its fault location problem challenging. This paper has contributed a novel solution for fault location in single-phase microgrids.

A feature specific to the fault location for locating a fault has been revealed, which is the approximated linear relation between the magnitude of transient signals induced by the fault observed by a sensor and the distance between the sensor and the fault location. The longer the distance between the sensor and the fault location, the larger the magnitude of the transient signals sensed.

After validating this feature through extensive simulations and theoretical studies, an appropriate algorithm for fault location based on the newly discovered relationship and information fusion from multiple sensors has been designed.

Finally the performance of the algorithm has been evaluated including its error analysis and robustness analysis. The average localization error obtained is in the range between 7% and 9%, which should satisfy the requirement of microgrid engineering practice and manifest the significance of the novel method for solving this challenging problem.

Researcher in [22] proposed a method to detect the faulted zone based on information provided by protective relays. With known faulty zone possibly help speed up the presented algorithm in the step of "fault location ranking" by removing candidate location(s) that may be excluded by their fault detection algorithm. Further research includes testing this method in field or on a test bed for single-phase microgrids with either centralized or decentralized control schemes. Future work also includes developing a software module based on this new method that can be integrated with energy management systems for microgrids.

Acknowledgment

The authors would like to thank Kwami Senam Sedzro and Huan Yang for their valuable comments to improve the quality of this manuscript.

Reference

[1] S. Bossart, "DOE Perspective on Microgrids," in *Advanced Microgrid Concepts and Technologies Workshop*, 2012.
[2] B.S. Hartono, Y. Budiyanto and R. Setiabudy, "Review of Microgrid Technology," in *International Conference on QiR*, 2013, pp. 127-132.
[3] S. Gopalan, V. Sreeram and H. Iu, "An Improved Protection Strategy for Microgrids," in *4th IEEE PES Innovative Smart Grid Technologies Europe (ISGT Europe)*, 2013, pp. 1-5.
[4] R. Majumder, A. Ghosh, G. Ledwith and F. Zare, "Operation and Control of Single Phase Micro-Sources in A Utility Connected Grid," in *IEEE Power and Energy Society General Meeting*, 2009, pp. 1-7.
[5] A. Khamis, A. Mohamed, H. Shareef, A. Ayob and M.S.M. Aras, "Modelling and Simulation of A Single Phase Grid Connected Using Photovoltaic and Battery Based Power Generation," in *Modelling Symposium (EMS)*, 2013, pp. 391-395.
[6] P. Jafarian and M. Sanaye-Pasand, "A Traveling-Wave-based Protection Technique Using Wavelet/PCA Analysis," *IEEE Transactions on Power Delivery*, vol.25, no.2, pp. 588-299, Apr. 2010.
[7] G. B. Ancell and N. C. Pahalawaththa, "Maximum Likelihood Estimation of Fault Location on Transmission Lines Using Travelling Waves," *IEEE Transactions on Power Delivery*, vol. 9, no. 2, pp. 680-689, Apr. 1994.
[8] IEEE Power Engineering Society, "IEEE Guide for Determining Fault Location on AC Transmission and Distribution Lines," *IEEE Standard C37.114-2004*, pp. 1-36, Jun. 2005.
[9] F.H. Magnago and A. Abur, "A New Fault Location Technique for Radial Distribution Systems Based on High Frequency Signals," in *Power Engineering Society Summer Meeting*, 1999, vol. 1, pp.426-431.
[10] A. Borghetti, S. Corsi and C.A. Nucci, "On the Use of Continuous-wavelet Transform for Fault Location in Distribution Power Systems," in *International Conference on Electrical Power and Energy Systems*, 2011, pp. 142-136.
[11] Fernando H. Magnago and Ali Abur, "Fault Location Using Wavelet Packets," *IEEE Transactions on Power Delivery*, vol. 13, no. 4, pp. 2575-2579, Oct. 1998.
[12] S.M. Brahma, "Fault Location in Power Distribution System with Penetration of Distributed Generation," *IEEE Transactions on Power Delivery*, vol. 26, no. 3, pp. 1545-1553, Jul. 2011.
[13] L.A.C. Lopes and S. Huili, "Performance Assessment of Active Frequency Drifting Islanding Detection Methods," *IEEE Transactions on Energy Conversion*, vol. 21, no. 1, pp. 171–180, 2006.
[14] G.K. Hung, C.C. Chang and C.L. Chen, "Automatic Phase-shift Method for Islanding Detection of Grid Connected Photovoltaic Inverters," *IEEE Transactions on Energy Conversion*, vol. 18, no. 1, pp. 169–173, 2003.
[15]M. Ropp, J. Ginn, J. Stevens, W. Bower and S. Gonzalez, "Simulation and Experimental Study of The Impedance Detection Anti-islanding Method in the Single-inverter Case," in *Proceedings of IEEE Photovoltaic Energy Conversion Conference*, May 2006, Vol. 2, pp. 2379–2382.
[16] G. Hernandez-Gonzalez and R. Iravani, "Current Injection for Active Islanding Detection of Electronically-interfaced Distributed Resources," *IEEE Transactions on Power Delivery*, Vol. 21, No. 3, pp. 1698–1705, 2006.
[17] E. Casagrande1, W.L. Woon, H.H. Zeineldin and N.H. Kan'an, "Data Mining Approach to Fault Detection for Isolated Inverter-based Microgrids," *IET Proceeding on Generation, Transmission & Distribution*, vol. 7, pp. 745–754, 2013.
[18] S. A. Saleh, R. Ahshan, M.A. Rahman, M.S.A. Khaizaran and B. Alsayed, "Implementing and Testing d–q WPT-Based Digital Protection for Micro-Grid Systems," in *Industry Applications Society Annual Meeting* , 2011, pp. 1-8.
[19] T. Basso and R. DeBlasio, "IEEE Smart Grid Series of Standards IEEE 2030 (Interoperability) and IEEE 1547 (Interconnection) Statue," In *Innovative Smart Grid Technologies (ISGT)*, 2012, pp. 1-7.
[20] A.G. Tsikalakis, N.D. Hatziargyriou, "Centralized Control for Optimizing Microgrids Operation," *IEEE Transactions on Energy Conversion*, vol. 23, no. 1, pp. 241-248, 2008.
[21] Allan Greenwood, "Electrical Transients in Power Systems" in *Wiley& Sons, Inc.* 2nd ed. New York, 1991, pp. 37-46.
[22] Y.Y. Hong, Y.H. Wei, Y.R. Chang, Y.D. Lee, P.W. Liu, "Fault Detection and Location by Static Switches in Microgrids Using Wavelet Transform and Adaptive Network-Based Fuzzy Inference System." *Energies 7*, no. 4: 2658-2675, 2014.

Jiajun Duan (S'2014) was born in Gansu, China, in 1990. He received his B.S. degree in Electrical Engineering from Sichuan University, Chengdu, China, in 2013. He is currently pursuing his M.S. degree in Electrical Engineering at Lehigh University, Bethlehem, PA and considering pursuing a PhD degree. His interest includes power system analysis, power electronics, control systems, renewable energy and smart grid.

Kaifeng Zhang (M'2010) received his Ph.D. degree from Southeast University, Nanjing, China in 2004 and joined the faculty of the same University. Currently he is a professor of Southeast University and a visiting scholar at Lehigh University,

Bethlehem, PA. His research interest includes power system modeling, control and dispatch, power market and microgrids.

Liang Cheng is an associate professor at Lehigh University. He has advised six Ph.D. students to their graduation and one postdoc. He has been the Principal Investigator (PI) and a Co-PI of fifteen projects supported by the U.S. National Science Foundation, Defense Advanced Research Projects Agency, Department of Energy, and state and industry sponsors. His current research focuses on ad-hoc/sensory networks and system instrumentation/analytics.